

LOW TEMPERATURE NATURAL GAS FUEL CELL BATTERY

W. J. Conner, B. M. Greenough, G. B. Adams

Materials Sciences Laboratory
Lockheed Palo Alto Research Laboratory
3251 Hanover Street, Palo Alto, California

INTRODUCTION

The Lockheed fuel cell battery is a model power-generating system of the indirect type using reformed natural gas and air. This model, with a gross power output of 430 watts, was constructed as part of a program to develop a reliable, low cost fuel cell system operating on these reactants.

Sulfuric acid is used as an electrolyte to provide compatibility with the carbon dioxide present in both the air and fuel, thus eliminating the need for a carbon dioxide scrubber and a hydrogen purifier. The operating temperature, 60°C, is too low for hydrogen reduction of the electrolyte, but sufficiently high to provide good electrolyte conductivity and a means for product water removal from the waste air. This low operating temperature allows the use of a wider range of construction materials than with higher temperature systems. These advantages, however, are partially offset by the relatively expensive electrode materials required for an acid electrolyte system.

A dual-matrix, circulating electrolyte design was selected for this battery because of its reliability and favorable operating characteristics. Electrolyte is circulated between two porous matrices which are contiguous to the operating electrodes. Thus, water balance and temperature control in each cell is simplified, and hazardous cross leakages of reactant gases is prevented; failure of one matrix does not result in a catastrophic reaction between fuel and oxidant. Electrolyte is conditioned thermally and for water balance externally to each cell in a heat exchanger and water feed system to provide a completely controlled cell, regardless of cell load. This conditioning is done automatically and reliably with minimal parasitic power loss.

The battery operates at ambient pressure and employs a novel air feed system. Pressure drops have been minimized with an open manifold system using low-power blowers to provide adequate air circulation. Reformate is also fed at low pressure to operate the system directly from a three-stage natural gas reformer which draws fuel from a conventional natural gas supply. Gas-liquid differential pressure regulation is achieved by maintaining a siphon action in the pumping of the electrolyte.

System reliability is increased by exclusive use of o-ring seals to eliminate leakage of corrosive electrolyte and hazardous fuel mixture. Battery control is automatically maintained by a safety system which effects system shutdown when triggered by any one of a number of signals indicating abnormal operation. The unit is completely self-contained, requiring only fuel, room air, and water for operation, and an inert purge gas for start-up and emergency shutdowns. A start-up battery is disconnected as soon as electrolyte, fuel, and air are distributed to the cells.

These and other technical advances resulting from Lockheed's fuel cell research and development programs are incorporated as design and operating features. This model provides an effective test bed for studying operational problems and delineating areas for further research and development.

BATTERY CONSTRUCTION AND OPERATION

Cell Reaction. A portion of the free energy of the reaction of hydrogen and oxygen to form water is converted into electrical energy in each cell. Hydrogen for this reaction is supplied as reformat from a three-stage natural gas reformer.* The reformat is approximately 90 percent hydrogen, 19.7 percent carbon dioxide, 0.3 percent methane and 10 parts per million carbon monoxide. Oxygen is supplied to the cell by blowing a stream of air over the oxygen electrode.

Cell Design. A cell is made up of two electrodes, fuel, air, and electrolyte spacer plates, matrix material, and support screens. The active material used for electrodes is designated RA-1 for anodes and AA-2 for cathodes.** Both types are fabricated on expanded tantalum mesh. The electrodes, 145 square centimeters in active area, are stretched flat by a special technique and are spot welded to a thin (2.5 mm) formed tantalum rim. Coarse, expanded-tantalum grids are spot-welded to the rim to provide a supporting structure for the thin electrode material. This rim and screen combination provides a means for current take-off. The anode is carbon monoxide resistant, and operates efficiently over long periods at 60°C in the presence of trace amounts of carbon monoxide.

Spacer plates are made of a corrosion and heat-resistant epoxy resin cast by a closed-mold process. All of the spacers contain o-ring sealed peripheral manifolding for fuel and electrolyte flow. The air spacer is open on two sides to permit blower air to pass uniformly across the cathode surface. Ports for electrolyte and fuel flow are cast into the appropriate plates. Each matrix, with support screen, is held in place in recessed steps cast into the electrolyte spacer. Assembly of the stack is simplified by integral pins on the electrolyte spacer which fit and lock contiguous plates during the stacking operation at assembly. Each fuel spacer is designed to accommodate two anodes and each air spacer, two cathodes. This design feature simplifies gas spacer fabrication and saves weight and volume in the assembled bank. Intercell connections are made externally to each cell with the extended electrode rim.

*Institute of Gas Technology, Chicago, Illinois.

**American Cyanamid Company, Wayne, New Jersey.

The electrolyte, 25 weight percent sulfuric acid maintained at 60°C, is circulated through each cell between two sheets of asbestos matrix material* contiguous to each electrode. These thin, porous matrices, filled with electrolyte, have a low specific resistance and provide impermeable barriers to the reactant gases. The gas-liquid interface is maintained at each electrode over a wide range of gas-liquid differential pressures. A nominal 10 inches of water gas-over-liquid differential pressure is maintained to prevent electrode flooding.

Module Design. The fuel cell battery consists of three 16-cell modules. One of these modules is shown in different views in Figures 1, 2, and 3. Figure 1 shows the inlet-air side of the module. The open edges of the air spacers and the inter-cell connectors are visible in this view. In Figure 2, the module has been rotated 180 degrees to show the exit-air side of the module. The electrical wiring seen in these figures is used to read individual cell voltages within the module. Series electrical connections are made by connecting extensions of the electrode rims as shown.

Shown in Figure 3 is one of the transparent end-plates through which the fuel spacer for the end cell is visible. The vertical strips inside the space are Viton o-ring stock which serve to direct the fuel flow over the electrode surface and to apply pressure against the electrode to insure good contact between the electrode and its matrix. The o-ring material, because of its resiliency, has a spring-like action which takes up assembly tolerance within the module. Each gas space within the module contains these strips, but in the air spaces they are placed horizontally so as not to obstruct air flow through the module. As the module is shown in Figure 3, electrolyte enters at the bottom of the front end-plate, is manifolded for parallel flow up from the bottom of each electrolyte spacer, and is again manifolded to leave the module at the top of the rear end-plate. With similar manifolding, fuel flows in the reverse direction, entering at the top of the rear end-plate and leaving the module at the bottom corner of the front end-plate.

A low-power, low-pressure fan** provides air flow for each module. The pressure drop which results from blowing air through the module is considerably smaller than the pressure drop for manifolding. As a result of using this air cross-flow technique, a low-power blower is adequate to provide air for the fuel cell reaction and excess air in sufficient quantity to contribute to the cooling of the cell and to remove product water. The air is directed through epoxy-fiberglass ducts into the modules. As it discharges from the module, it passes into a cold-surface chamber on the exit side of each module where product water is condensed from the air stream. In Figure 4, the inlet air duct is shown on the left side of the module; the exit duct with its water-cooled cold surface and exhaust stack is on the right side.

The air filters are shown in Figure 5. The air blowers are mounted inside the ducts directly behind these filters.

*Johns Mansville Company, New York City, New York.

**Rotron Manufacturing Company, Woodstock, New York.

Battery Design. The three modules are assembled on a polyester-fiberglass rack measuring $24 \times 24 \times 40$ inches. Total system weight including auxiliaries and controls, but without reformer, is 223 pounds. The auxiliary system is located within this rack and is connected as shown in Figure 6. Figures 4, 5, and 7 illustrate the spatial relationships of the system components.

Materials of Construction. Materials used in the system have been tested for their resistance to the corrosive environment of hot sulfuric acid. Plastics are employed extensively; polypropylene plumbing, epoxy cell parts, polycarbonate reservoirs and module end-plates, epoxy-fiberglass ducts, and polyester-fiberglass system rack. Tantalum is used wherever a metal is required in direct contact with the electrolyte, such as the electrode rims and matrix support screens.

Electrolyte Circulation. The electrolyte circulation system includes a pump, heat exchanger, flow meters, flow control valves, and a liquid reservoir and water balance system.

The centrifugal, magnetically driven pump* is constructed with only polypropylene and Teflon in contact with the hot acid electrolyte. Panel mounted flow meters register the electrolyte flow, and plastic valving controls the flow distribution to the three modules.

Thermal Control. The heat exchanger,** a shell and tube type, is constructed so that the only exposed materials are Teflon and polycarbonate. Depending on the heating or cooling requirements, hot or cold tap water is admitted to the shell side of the heat exchanger. Hot water brings the system up to temperature, after which the hot water valve is interlocked in an off position, and control is maintained by supplying cold water on demand. A thermostat in the electrolyte triggers the appropriate heating or cooling water solenoid valve.

Water Balance. The electrolyte reservoir, as shown schematically in Figure 6, consists of a series of cylindrical polycarbonate chambers where electrolyte is returned from the modules and water balance is automatically maintained. Water condensed from the air ducts returns to holding chamber (A) through a filter. Excess condensate is discharged to the drain through an overflow tube. If insufficient water is condensed, a float admits make-up water from an external source by opening the distilled water solenoid valve. All of the spent fuel, laden with water vapor, passes through chamber (B) where water condenses on the walls. The liquid level in this vessel rises until the float valve opens to drop the condensed water into electrolyte compartment (C). A water seal maintained by the float prevents mixing of the spent fuel with air. Electrolyte passes through compartments (C), (D), and (E). The first of these, (C), is a settling chamber which serves to free entrapped gas from the electrolyte. The electrolyte discharges from compartment (C) into (D) which contains a float valve. The initial loading of electrolyte lifts this float valve upwards to the sealed position preventing water from flowing from chamber (A) mounted above. Since

*Micropump Corporation, Concord, California.

**E. I. DuPont De Nemours & Company, Wilmington, Delaware.

excess water is removed from the electrolyte by the air stream, the operation of the cell results in a decrease in electrolyte volume as water is evaporated. This volume change is sensed by the float valve which drops, unseating the valve. Water then flows into this compartment from the air condensate chamber A. When sufficient water has been added to return the float valve and volume to the original level, the valve seals, cutting off water flow. In actual operation, this valve modulates at a point where water is continuously added to make up for the excess that is removed. The reconstituted electrolyte then issues into compartment (E), where a high-low reservoir level sensor detects electrolyte flow irregularities and signals system shutdown if an unsafe condition exists. The electrolyte then is withdrawn by the pump and is circulated through the system.

System Startup. Gas service on the fuel side of the system consists of hydrogen, reformat, and an inert gas, e. g., nitrogen, admitted automatically by solenoid valves. During start-up, the fuel cell system operates on hydrogen and air while the electrolyte is being heated. When the temperature reaches 50°C, the system automatically switches to reformat. This procedure is used to prevent carbon monoxide poisoning of the anode, a reaction which occurs more readily at lower temperatures.

The inert gas is provided as a purge which can be manually operated when the system is to be turned off, but which operates automatically in case of a safety shut-down or whenever the auxiliary power is disconnected.

Safety Features. The automatic safety shut-down is an important feature of the system. It consists of complete system shut-down and inert gas purge in response to a signal from the safety circuit. Low system differential pressure or a significant change in the electrolyte volume due to water imbalance triggers either the high or low level safety circuit in the reservoir. Over-heating of any one of the modules is also sufficient reason for shut-down and is sensed by a thermo-switch in the end fuel spacer of each module. Latching relays in the safety circuit provide control when triggered by any of these signals. These relays are latched into the "safe" position by a manually actuated electrical pulse and then require no electrical power until a safety signal latches the relay in the "unsafe" position actuating system shutdown. In this way, the safety circuit provides control without drawing electrical power.

Parasitic Power Requirements. Except for battery power required for operating auxiliaries during the first few minutes of start-up, the model system is self-sustaining. Figure 8 is a back view of the top section of the front panel showing the location of the electrical control circuits and the auxiliary power inverter. Auxiliary power inversion permits the use of AC motors rather than DC motors with their life-limiting brushes and hazardous brush sparking. The DC to AC inverter operates on fuel cell power, and provides AC power to the air blowers and electrolyte pump. To maintain constant output voltage to the auxiliaries with varying external loads, an automatic voltage selector switch places the required number of cells across the auxiliary power buss to maintain correct voltage within 0.8 volts.

Low-power relays and indicator lights are used to conserve auxiliary power; the maximum auxiliary load at any given time is 58 watts including all power for the blowers, pump, inverter, relays, solenoid valves, and controls. This figure would increase to approximately 70 watts for a 2 kilowatt battery. The front control panel is shown in Figure 9. All of the cell voltages may be measured from the front panel to provide for an easy assessment of cell performance. Various temperatures may be read on the front panel for ready assessment of system operating conditions. The electrical control system is built as a module for easy removal and maintenance.

ELECTROCHEMICAL PERFORMANCE

Initial test work was conducted on cells having an active electrode area of 18 square centimeters. A cell with 90 square centimeters active electrode area was assembled and tested as an intermediate to the final design. Polarization and long-term performance data from these cells provided the scale-up information necessary to design a large cell with 145 square centimeters active electrode area. This cell size was used in the multicell modules.

Long-Term Performance. Long-term performance of the small cells was of particular interest in determining the mode of cell failure, if any. Anode and cathode performance with time was measured versus a hydrogen reference. The results of one 950-hour test are shown in Figure 10. The anode, operating at 60°C on reformat, is quite stable over this long period of operation; the apparent degradation is 10 mV per 1000 hours of operation. The cathode, operating on room air, degrades rapidly in the first 50 hours. This rate then slows and at about 400 hours stabilizes to about 10 mV per 1000 hours. A brief interruption of the load (which occurred at 580 hours) improves the cathode potential (anodic change is negligible). On load again, the cathode degrades rapidly, and after about 48 hours, the cathode potential is the same as it was prior to the interruption. This test cell, representative of a large number of long-term test cells, was operated continuously in an automated test facility.

Figure 11 illustrates a 300 hour performance test conducted on a single large cell similar to those used in the multicell bank. A problem encountered in maintaining the cell temperature in the early portion of this test resulted in unsteady anode performance during this period. At 115 hours, a polarization run (Figure 12) was made, and the temperature control was modified and improved. The latter portion of this test is characteristic.

Cell Voltage-Current Characteristics. The polarization diagram for the large cell is presented in Figure 12. A resistance-free curve is plotted to show the effect of cell resistance on cell performance. Also included is a plot of total power output from the cell. The dashed voltage line illustrates an average cell voltage found in an operating 16-cell module.

In a cell with a carbon monoxide resistant anode, the anodic polarization initially and over long periods of time is low, unless the anode is poisoned by a fuel gas with a high carbon monoxide content or decomposition products from the electrolyte (hydrogen sulfide). This may happen when a cell is operated at too high a temperature or when certain materials of construction not compatible with hot sulfuric acid are used.

The cathode, on the other hand, is rather severely polarized and controls cell voltage at low current densities. As the load is increased, the cathode potential stabilizes and cell resistance then controls cell potential. Even though precautions were taken in the design, fabrication, and assembly of the large cell and modular assembly, the unit cell specific resistance is double that of the small cell. Current development is directed to the definition and further reduction of this increased resistance.

Air-Fuel Flow Rates. A series of tests were conducted with the large cell to define reactant flow rates required to support cell operation at different current densities. Figure 13 illustrates the performance of the anode with reformat. This electrode requires a fuel flow rate only slightly in excess of stoichiometric at all current densities. However, at low current densities with stoichiometric flow, anodic polarization increases slightly due to poor gas flow distribution. The non-reactants in the fuel tend to mask off portions of the anode at low flow rates. At higher current densities with stoichiometric flows, the higher gas flow helps to sweep non-reactants out of the stagnant areas of the anodic gas spacer. Because of this, the anode operates for extended periods at high current densities at the stoichiometric fuel flow rate because of the net purging of the fuel spacer with the carbon dioxide and other non-reactants introduced into the cell as part of the fuel.

The cathode can be operated at stoichiometric rates up to 50 mA/cm^2 . At higher current densities, cell performance drops off drastically, but air flow rates three times stoichiometric or greater will support all current densities through (150 mA/cm^2). These data are presented in Figure 14.

An analysis was made of the air flow through a 16-cell module with a fan* which has a free air delivery of 50 cubic feet per minute. The volumetric flow through each air spacer was calculated from velocity probe measurements made at the discharge of each cell spacer. The fan draws air through a polyurethane foam filter and blows air through the module. No distribution device is used in this configuration, and the uneven flow pattern across the face of the module is shown in Figure 15. The lower flow rate through the center cells is caused by zero air flow through the hub of the fan which is located directly in front of cells 7-8 and 9-10. Lines of constant 1 and 10 stoichiometric flow rates are shown in Figure 15 to provide a reference. It can be seen that this fan and distribution configuration is adequate since a minimum three stoichiometric flow requirement is met. The disadvantages of higher air flow rates are the extra load impressed on the air condenser and water balance control system and the lower cell temperature of high-flow-rate cells. If, with the fan used, air flow is decreased further (by restricting the air inflow), the edge-to-center air flow distribution pattern becomes more distorted. It is therefore imperative that air flow through

*Rotron Sentinel Fan with a 745 motor.

the cells be high enough for good cell performance, but not too high for good water balance control.

The vent stack height used in the multicell system provides sufficient updraft in a module without fan and filter to support the bank at 100 mA/cm^2 at 60°C .

Total System Performance. The assembled, three module, 48 cell battery described in this paper exhibits the performance characteristics shown in Figure 16. The system has been operated under a variety of loads with completely automatic control. The system operates efficiently on reformat and room air to give the power output shown in Figure 16. Little excess fuel is required to maintain a steady load. Sufficient air flow is obtained from 5 watt fans. Work is continuing to define the limiting parameters in the cell performance in order to increase total output from the battery.

FUTURE IMPROVEMENTS

One area for improvement in this system is in the design of a larger, and less costly cell. A larger cell would allow a reduction in the number of cells per module for the same power output. Improvements would include reduced cell resistance, increased ratio of active to inactive area in cell cross section, improved structural integrity, and the development of mass production techniques for cell parts. Electrodes with low catalyst loading would be incorporated in the design to reduce electrode unit costs further.

The cell and module design would also be optimized to maximize performance with respect to minimal weight and volume. This would be achieved with an improved electrode and matrix containment design which would eliminate tantalum at certain points in the cell where it is now used.

Another area for improvement in this system is in further reduction of parasitic power requirements. Thermal control can be achieved by cooling with air instead of water. This can be done with a bypass air cooling system which allows cooling air to flow through or around each cell, regulated by a damper under passive control. Use of a single blower with improved air distribution for larger modules will reduce parasitic power requirements further.

These and additional improvements should establish this system as an efficient, economical power source for future domestic and ground-based military applications.

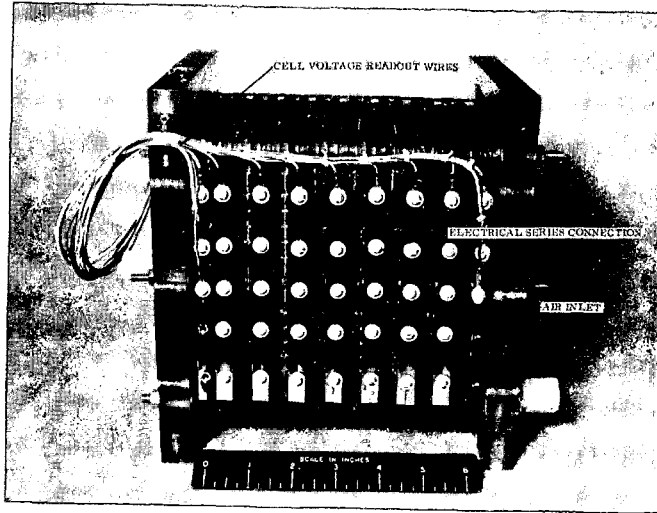


Fig. 1 Sixteen Cell Module - Inlet Air Side

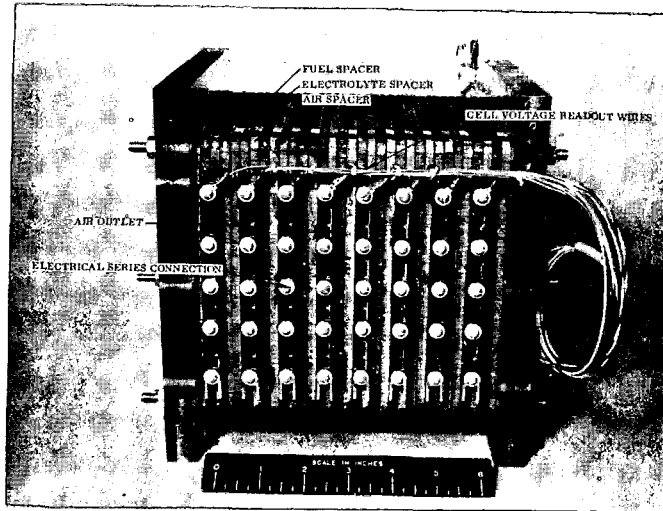


Fig. 2 Sixteen Cell Module - Exit Air Side

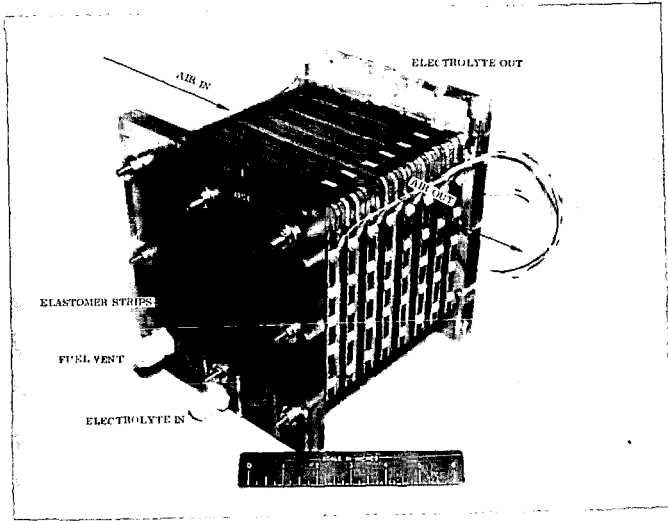


Fig. 3 Sixteen Cell Module

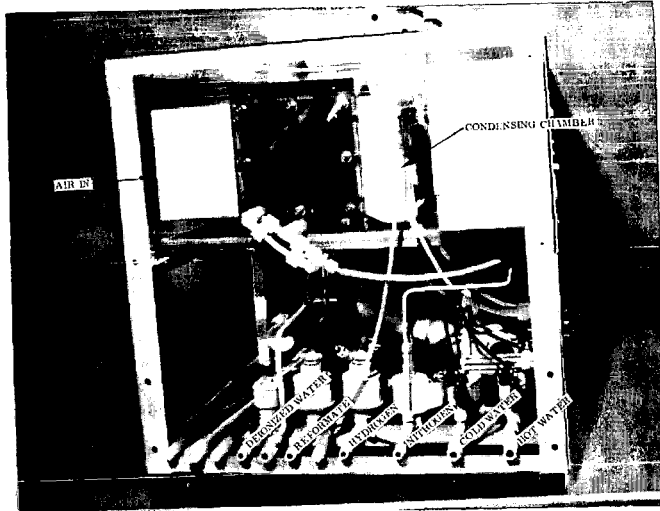


Fig. 4 Fuel Cell System - End View

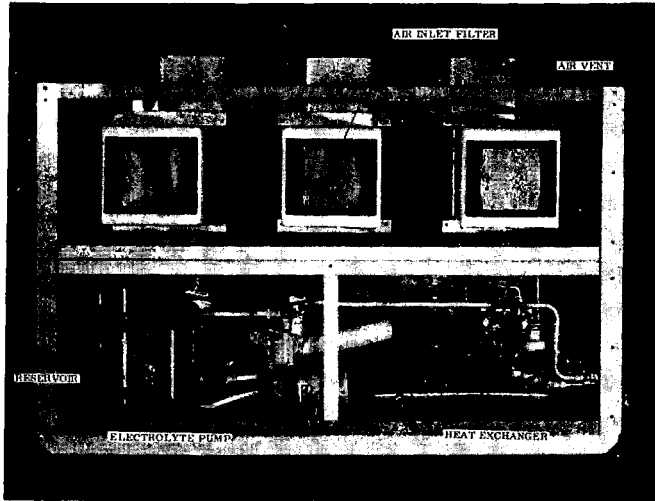


Fig. 5 Fuel Cell System - Rear View

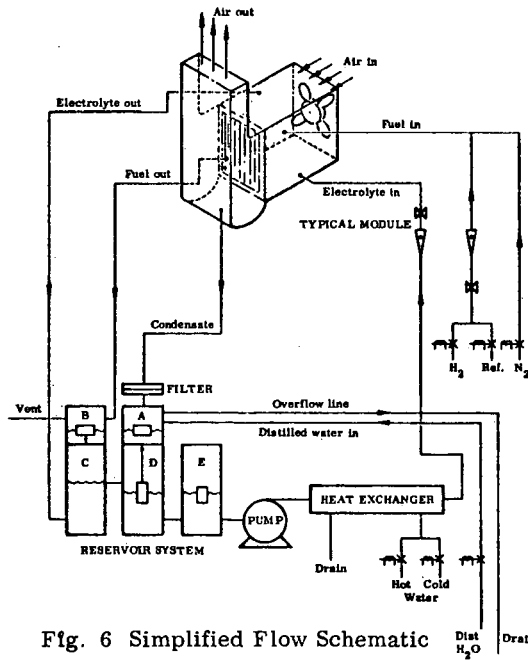


Fig. 6 Simplified Flow Schematic

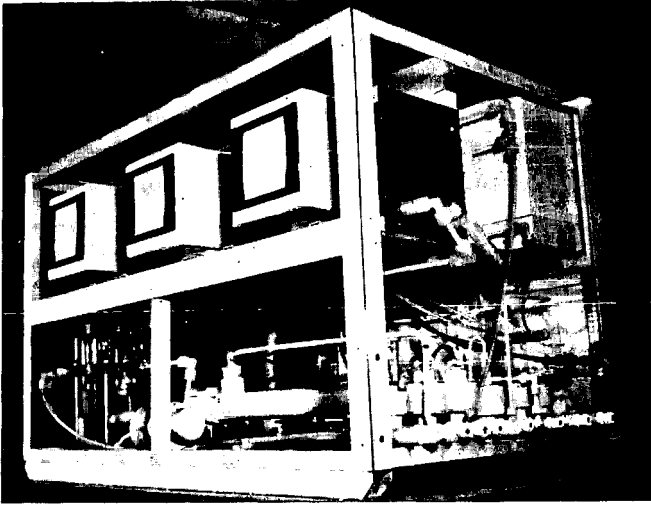


Fig. 7 Fuel Cell System

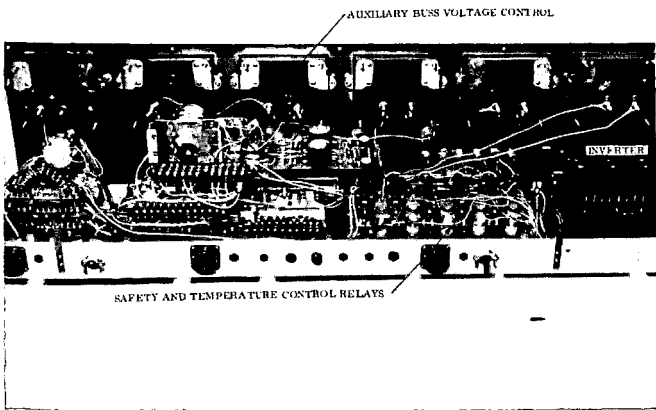


Fig. 8 Electrical Controls

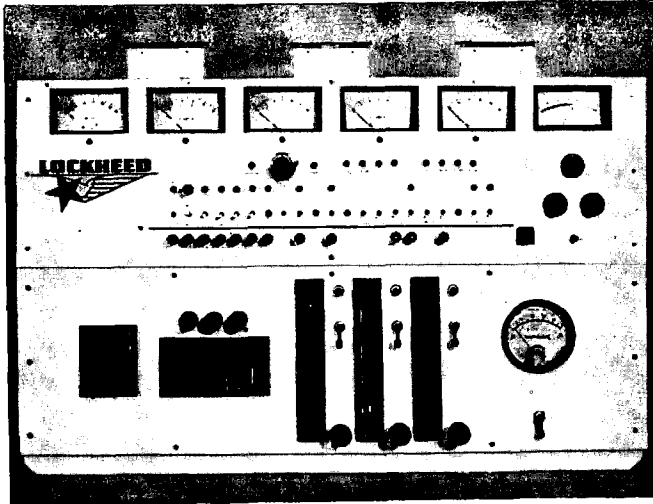


Fig. 9 Fuel Cell System - Front Panel

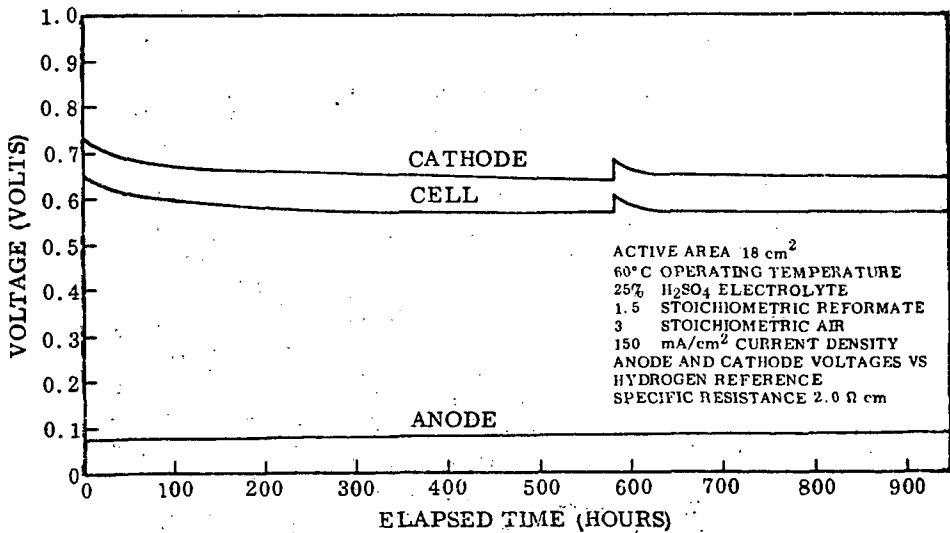


Fig. 10 Long-Term Performance of a Small Cell

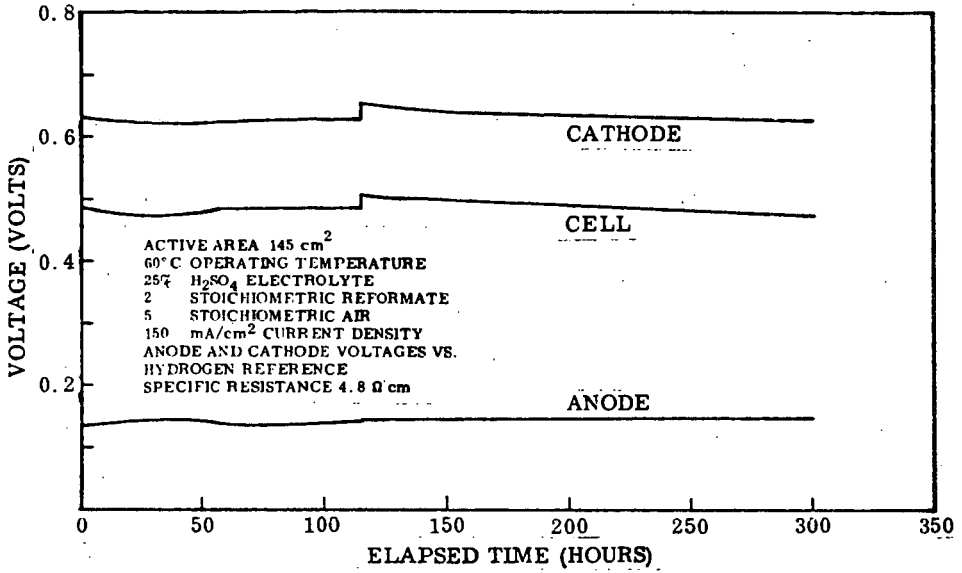


Fig. 11 Long-Term Performance of a Large Cell

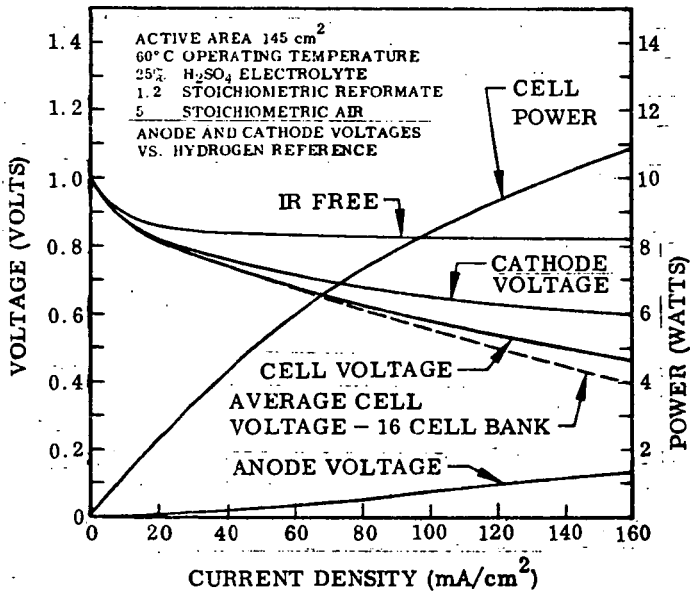


Fig. 12 Performance Characteristics of a Large Cell

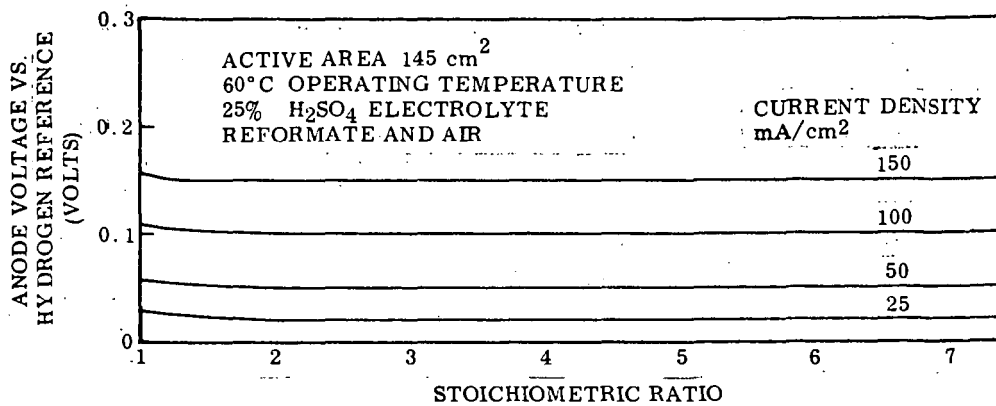


Fig. 13 Variation of Anode Voltage With Fuel Flow Rate

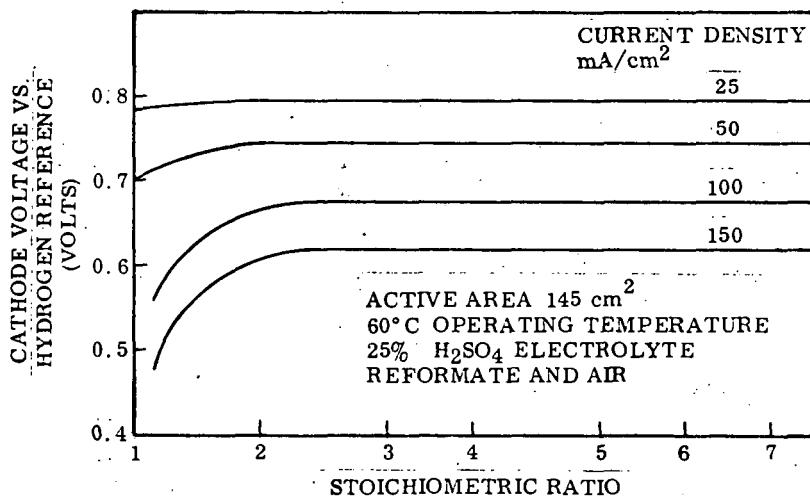


Fig. 14 Variation of Cathode Voltage With Air Flow Rate

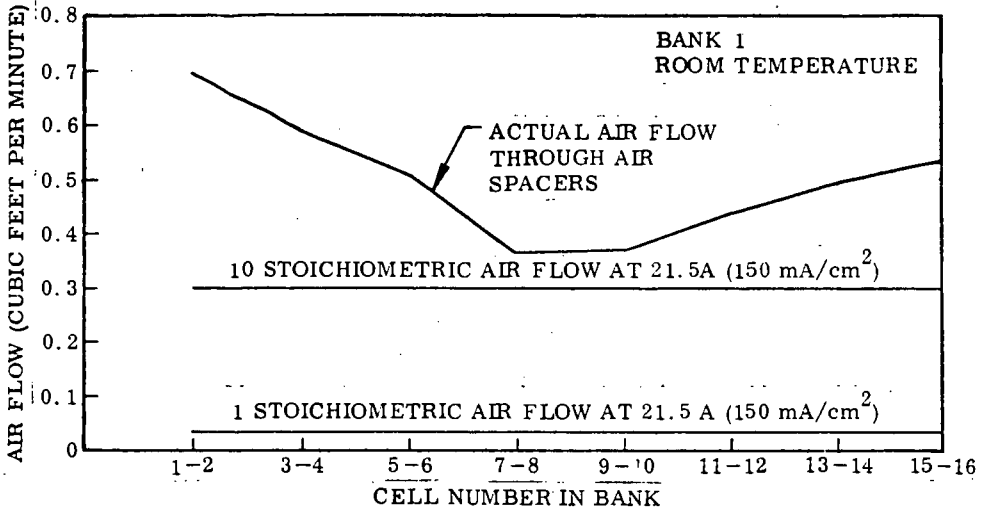


Fig. 15 Variation of Air Flow in Air Spacers of Multi-cell Bank

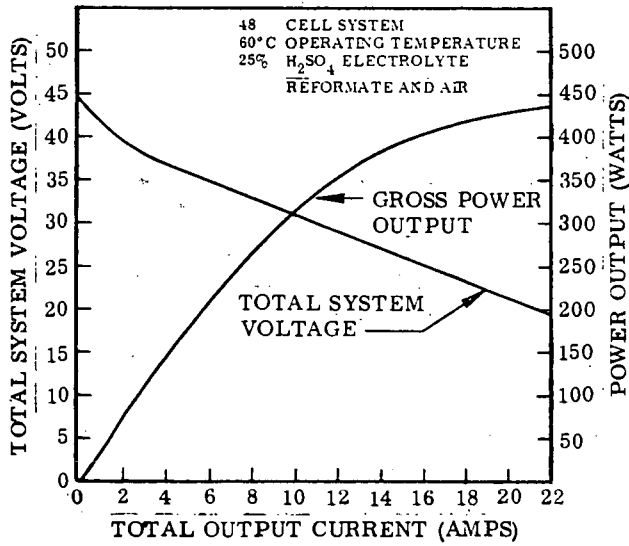


Fig. 16 Performance of a Multi-cell Bank